Parameterizing the Dependence of Surface Albedo on Solar Zenith Angle Using Atmospheric Radiation Measurement Program Observations

F. Yang
Environmental Modeling Center
National Centers for Environmental Prediction
Camp Springs, Maryland

Abstract

This study evaluates the parameterization of the dependence of surface albedo on solar zenith angle (SZA) over snow-free land surface used by the National Centers for Environmental Prediction Global Forecast Systems (GFS) and those derived from the moderate resolution imaging spectroradiometer satellite observations as described in two recent studies. The influence of cloud cover on surface albedo is also examined. The intensive ground observations of surface shortwave fluxes and cloud covers made by the Atmospheric Radiation Measurement (ARM) Program at the United States Southern Great Plains (SGP) site and at the Tropical Western Pacific (TWP) locale's Manus and Nauru Islands in 1997 – 2004 are used for the investigation. The albedos for the direct and diffuse solar beams are considered separately. The diffuse-beam albedo is first derived from a subset of the ARM Program samples under overcast conditions and with the downward total flux being all diffuse. Then, it is used to divide the measured surface upward flux into two parts, one associated with the downward direct beam and the other with the downward diffuse beam for all samples. The direct-beam albedo is finally obtained using the first part of the upward flux and the downward direct-beam flux. It is further normalized either by the diffuse-beam albedo or by the direct-beam albedo at SZA=60°. The normalized albedo only varies with the SZA and is independent of the solar spectrum.

Results show that at the SGP site, while the diffuse-beam albedo prescribed in the GFS matches closely the ARM Program observed, the direct-beam albedo parameterized in the GFS largely underestimated at all SZA. The parameterizations derived from the moderate resolution imaging spectroradiometer products tend to underestimate the direct-beam albedo at large SZA and slightly overestimate at small SZA. The influence of cloud cover on surface albedo is negligible in comparison with the albedo variation with the SZA. This study recommends that in weather and climate models the direct-beam albedo over snow-free land surfaces be parameterized as a product of the direct-beam albedo at SZA=60° (or the diffuse-beam albedo), which can be obtained from satellite observations and be prescribed in the model differently for different surface types and/or seasons, and a universal function that depends only on the SZA.

Introduction

Surface albedo is one of the most important parameters that affect the earth's surface energy budget. It is one major source of uncertainties for radiative transfer calculations. Land surface albedos over both bare soil and plant canopy have strong dependence on SZA and the surface characteristics. Since the surface types change considerably from place to place, it is formidable to develop different schemes to model the dependence of surface albedo on SZA for different surface types (Briegleb et al. 1986). Dickson (1983) described a scheme for a semi-infinite canopy consisting of randomly oriented leaves, that is,

$$\alpha(\theta) = \alpha_0 \cdot \frac{1+d}{1+2d\cos(\theta)}, \quad (1)$$

Where θ =SZA, $\alpha\theta$ is surface albedo at a given θ, α_0 the albedo at cos(θ) = 0.5, and d is a constant. This scheme was intended for broad-band solar flux and made no differentiation between direct and diffuse beams.

In its subsequent applications this scheme was modified and expanded to parameterize the albedo-SZA relation over all snow-free land points (Briegleb et al. 1986; Briegleb et al. 1992; Pinker and Laszlo 1992; Hou et al. 2002). For example, Briegleb et al. (1992) added to the scheme the spectral dependence of surface albedo on SZA for the then National Center for Atmospheric Research (NCAR) Community Climate Model (CLM). They set a_0 differently for the visible (0.2-0.7 μm) and near-infrared (0.7-5.0 μm) bands and differently for different land surface types based on various observations, and further prescribed d to 0.4 for arable land, grassland and desert over which the SZA dependence of surface albedo is strong and d to 0.1 for all other land surface types over which the dependence of surface albedo on SZA is weak. Pinker and Laszlo (1992) used the same scheme as described in Briegleb et al. (1992) but with finer spectral resolution to compute surface albedo as the first guess for satellite retrieval of surface radiative fluxes. Briegleb et al. (1992) and Pinker and Laszlo (1992) did not differentiate the direct and diffuse beams for the surface downward solar fluxes and used the same relation for both. Considering that surface albedo for the diffuse beam does not depend on the solar spectrum, Hou et al. (2002) further modified the scheme described in Briegleb et al. (1992) and only applied it for computing the direct-beam surface albedo, that is,

$$\alpha_{dir}(\theta,\lambda) = \alpha_{diff}(\lambda) \cdot \frac{1+d}{1+2d\cos(\theta)}, \quad (2)$$

where $\alpha_{diff}(\lambda)$ is the diffuse-beam albedo prescribed differently for the ultraviolet and visible band (0.175-0.7 μm) and the near-infrared band (0.7-10 μm) and differently for different surface types. $\alpha_{diff}(\lambda)$ also varies with the season. It was derived from the land-use and surface albedo dataset given by Matthews (1983) and Matthews (1984). This scheme is still being used in the operational National

Centers for Environmental Prediction (NCEP) GFS to compute surface radiative fluxes, although in the near future it will be replaced by the more complex surface albedo algorithm imbedded in the NCEP "Noah" Land Surface Model (Ek et al. 2003; Mitchell et al. 2004).

Please note that in modern land-surface models (e.g., Bonan 1996; Koster et al. 2002; Dai et al. 2003; Ek et al. 2003] surface albedos are usually computed separately for bare soil and vegetation and then combined together. The albedo for bare soil depends on soil moisture and soil color types, and does not depend on the SZA. The albedo for vegetation depends on vegetation characteristics such as leaf and stem area index and vegetation optical property, and on SZA for the solar direct beam. It is either parameterized by a simplified two-stream solution under certain constraints (e.g., Dai et al. 2003) or explicitly resolved by canopy radiative-transfer equations (Bonan 1996; Dai et al. 2004; Oleson et al. 2004). For the schemes described in Briegleb et al. (1992) and Hou et al. (2002), although vegetation albedo is not explicitly represented, it can be regarded as being implicitly resolved by the prescribed surface albedo α_0 or $\alpha_{diff}(\lambda)$, which does vary with surface soil and vegetation types.

The Dickson (1983) parameterization and its variations (Briegleb et al. 1992; Hou et al. 2002) were derived from limited observations. Its accuracy has been a constant subject of discussion. In particular, there is a lack of observations with sufficient solar angular resolution for verifying the SZA dependence (Lyapustin 1999). In recent years, significant progress has been made in the modeling of land-surface albedo since the high-quality fine-resolution satellite measurements from the Moderate Resolution Imaging Spectroradiometer (MODIS; Schaaf et al. 2002; Gao et al. 2005) became available. For example, using the MODIS Bidirectional Reflectance Distribution Function (BRDF) albedo algorithm and data Wang et al. (2006) derived a two-parameter scheme for computing the direct-beam (black-sky) albedo over land and its SZA dependence for climate and weather forecast models, that is,

$$\alpha_{dir}(\theta,\lambda)=\alpha_{dir}(60^o,\lambda)\cdot\left\{1+B_1\cdot\left[g_1(\theta)-g_1(60^o)\right]+B_2\cdot\left[g_2(\theta)-g_2(60^o)\right]\right\}, \quad (3)$$

where $\alpha_{dir}(\theta, \lambda)$ is the direct-beam albedo for a given θ and for either the visible band or the near-infrared band, $a_{dir}(60°, \lambda)$ is the direct-beam albedo at 60° and varies with season and vegetation types. The functions $g_1(\theta)$ and $g_2(\theta)$ are from the MODIS algorithm (see Wang et al. 2006). The parameters B_1 and B_2 also vary with vegetation types. Wang et al. (2006) also parameterized the albedo $\alpha_{dir}(\theta, \lambda)$ following the Dickson (1983) approach, that is,

$$\alpha_{dir}(\theta,\lambda)=\alpha_{dir}(60^o,\lambda)\cdot\frac{1+c}{1+2c\cos(\theta)}. \quad (4)$$

Here the parameter c is defined differently from the parameter d in Eq. (2). It is obtained by minimizing the difference between the MODIS albedo and the albedo computed from Eq. (4) over all SZA in a given period for each vegetation type. Wang et al. (2006) found that c changes considerably among the vegetation types and is very different from the two constants given in Briegleb et al. (1986).

The schemes described thus far (Eqs. 1-4) parameterize surface albedo as a function of SZA and vegetation types. They do not treat bare-soil albedo and vegetation albedo separately as most modern land-surface models do (e.g., Bonan 1996; Koster et al. 2002; Dai et al. 2003; Ek et al. 2003). Starting from the NCAR CLM surface albedo algorithm, Liang et al. (2005) developed a new dynamical-statistical albedo scheme for snow-free land surfaces using the MODIS reflectance and vegetation products along with soil moisture products from a land data assimilation system. The albedo over vegetation was separated from that over bare soil. Unlike the NCAR CLM in which the bare-soil albedo is a function of soil moisture and soil color types and does not vary with the SZA, Liang et al. (2005) parameterized the bare-soil albedo as a product of two terms, one is a function of soil moisture and the other a function of the SZA. The bare-soil direct-beam albedo (Eq.7 of Liang et al. [2005]) can be rewritten as

$$\alpha_{dir}(\theta,\lambda)=\alpha_{dir}(\lambda)|_{\mu=0,\vartheta=0}\left[1+C_{1,\lambda}\cos(\theta)+C_{2,\lambda}\cos^2(\theta)\right]\cdot F(\vartheta,\lambda), \quad (5)$$

where $F(\vartheta, \lambda)$ is a function of soil moisture (ϑ) and wavelength, $C_{1,\lambda}$ ($C_{2,\lambda}$) equals to –0.718 (0.346) for the visible band and –0.732 (0.362) for the near-infrared band, $\alpha_{dir}(\lambda)|_{\mu=0,\vartheta=0}$ is referred to as the maximum background soil albedo that varies with the land cover types and is defined differently for the visible and near-infrared bands. Liang et al. (2005) demonstrated that this new scheme remarkably improved the accuracy of surface albedo calculation in comparison with the one in the NCAR CLM. The dependence of bare-soil albedo on SZA is important and cannot be ignored as most current land-surface models do.

Remarkable progresses have been made using the MODIS products to understand the surface albedo characteristics and to improve the parameterization of surface albedo for numerical models (e.g., Lucht et al. 2000; Wang et al. 2004; Liang et al. 2005; Wang et al. 2006). However, the dependence of surface albedo on SZA derived from the MODIS data needs to be further examined. First, the MODIS data are not reliable near dusk or dawn for SZA greater than 70° ($\cos(\theta) < 0.34$) when atmospheric aerosol correction of the input data degrades and the BRDF models themselves grow weak (Liang et al. 2005). Second, the current available MODIS data are 16-day composite retrieved under clear-sky conditions. The 16-day mean diurnal cycle of SZA does not reflect the true SZA variation in a specific day at a given location. The MODIS clear-sky products can not answer how and if the surface albedo varies with the atmospheric conditions either. Using a comprehensive radiative transfer model Lyapustin (1999) simulated surface albedo for different land cover types under widely varying atmospheric conditions. He found that surface albedo indeed varies with atmospheric opacity, although this dependence is secondary compared to its variation with SZA and land cover types.

Therefore, to better understand the albedo-SZA relation it is desirable to have long-term measurements of surface solar fluxes that are accurate and of high solar angular resolution, especially at large SZA, under both clear and cloudy sky conditions. The U.S. Department of Energy's Atmospheric Radiation Measurement (ARM) Program (Stokes and Schwartz 1994; Ackerman and Stokes 2003) provided such a

unique opportunity for us to revisit the albedo-SZA relations described in Briegleb et al. (1992) and Hou et al. (2002) and recently derived from the MODIS products (e.g., Liang et al. 2005; Wang et al. 2006). The ARM Program was established in 1990 and has been making intensive and continuous measurements of surface solar radiative fluxes and atmospheric quantities at the ARM Climate Research Facility (ACRF) surface sites in the SGP site, and the North Slope of Alaska (NSA) and TWP locales. These measurements have been used in the past to improve our understating of the cloud-radiation interaction and to evaluate climate model simulations and satellite retrievals of surface radiaitve fluxes and albedo (e.g., Long and Ackerman 1997; Minnis et al. 1997; Li et al. 2002; Trishchenko et al. 2005). However, they have not been used to examine the albedo-SZA relation for the direct-beam solar fluxes. The ARM Program measures surface downward total and diffuse-beam solar fluxes and the upward (reflected) total solar flux. It is a question how to partition the reflected flux so as to derive the respective albedos for the downward direct and diffuse beams. A novel method will be introduced in this study to deal with this issue.

The purpose of this study is to make use of the extensive and long-term ARM observations of surface solar radiative fluxes and cloud conditions at the SGP site and the TWP Manus and Nauru islands to evaluate the albeo-SZA relations described above, and to improve these parameterizations if possible for climate and weather forecast models. We focus first on the ARM observations at the SGP site to establish the methodology. The ARM data collected at the TWP Manus and Nauru Islands will then be used for cross validation.

ARM Observation

The observational data used for this study (see Table 1) were obtained from the ACRF Data Archive (http://www.arm.gov/data/). For details about instruments, data processing and quality controls readers are referred to Shi and Long (2002) and the ARM website for radiative flux and to Clothiaux et al. (2001) for clouds. Based on the availability of both radiation

Table 1. ARM data streams and variables used for the study.

Data Stream	Site	Measurements Used for this Study	Data Frequency
Value-Added Best-Estimate Radiative Flux (BEFLUX)	SGP Central Facility	Surface downward total and diffuse shortwave fluxes, surface upward shortwave flux	1 minute
Ground Radiation Sensor (GNDRAD)	TWP Manus TWP Nauru	Surface upward shortwave flux	1 minute
Sky Radiation Sensor:(SKYRAD)	TWP Manus TWP Nauru	Surface downward total and diffuse shortwave fluxes	1 minute
Active Remotely-Sensed Clouds Locations (ARSCL)	SGP Central Facility TWP Manus TWP Nauru	Cloud base and top heights	10 seconds

and cloud products, this study uses the data in the 1997 – 2004 period at the SGP Central Facility (CF) and the data in the 2001 – 2004 period for the TWP Manus and Nauru Islands. A solar positioning algorithm (available from http://www.squ1.com/) was used to compute SZAs at one-minute temporal resolution in accordance with the time and locations of the observations at the three ACRF research sites. We found that the SZA data included in the BEFLUX data stream (Table 1) are not accurate before 2001. The ARM data streams for the TWP sites do not have the SZA information.

The radiation and cloud data we acquired from the ACRF Archive are in one-minute and ten-second temporal resolutions, respectively. For this study, both data and the SZA were resampled as five-minute means. The ten-second ARSCL cloud-base distributions in each five-minute period were used to derive cloud occurrence frequency (cloud cover). We also tested one-minute and ten-minute samplings and obtained almost identical results. One-hour sampling degrades the solar angular resolution. We opted to use the five-minute sampling to take advantage of the high solar angular resolution as yet to keep the multi-year ARM data manageable.

As an example, we show in Figure 1a the diurnal distribution of surface total albedo at the SGP CF (36.6°N, 97.5°W) in 2003. Here, total albedo is defined as the ratio between the surface upward and the surface downward total shortwave fluxes. The radiation instruments at the SGP CF site are situated on a pasture field. The albedo varied with the time of the day and the season, and was usually larger at dawn and dust than at noon. It was in the range of 0.1 ~ 0.3 except for the days when the ground was covered by snow (see the yellow and red shadings in Figure 1a). For this study, data samples with surface total albedo greater than 0.4 were excluded from the analysis. We further excluded those samples that had the downward or upward flux smaller than 10 W/m^2, which is close to the upper bound of the ARM radiation instrument uncertainty (http://www.arm.gov). There are a total of 245,606 qualified samples at the SGP CF from the 1997-2004 period (see Table 2).

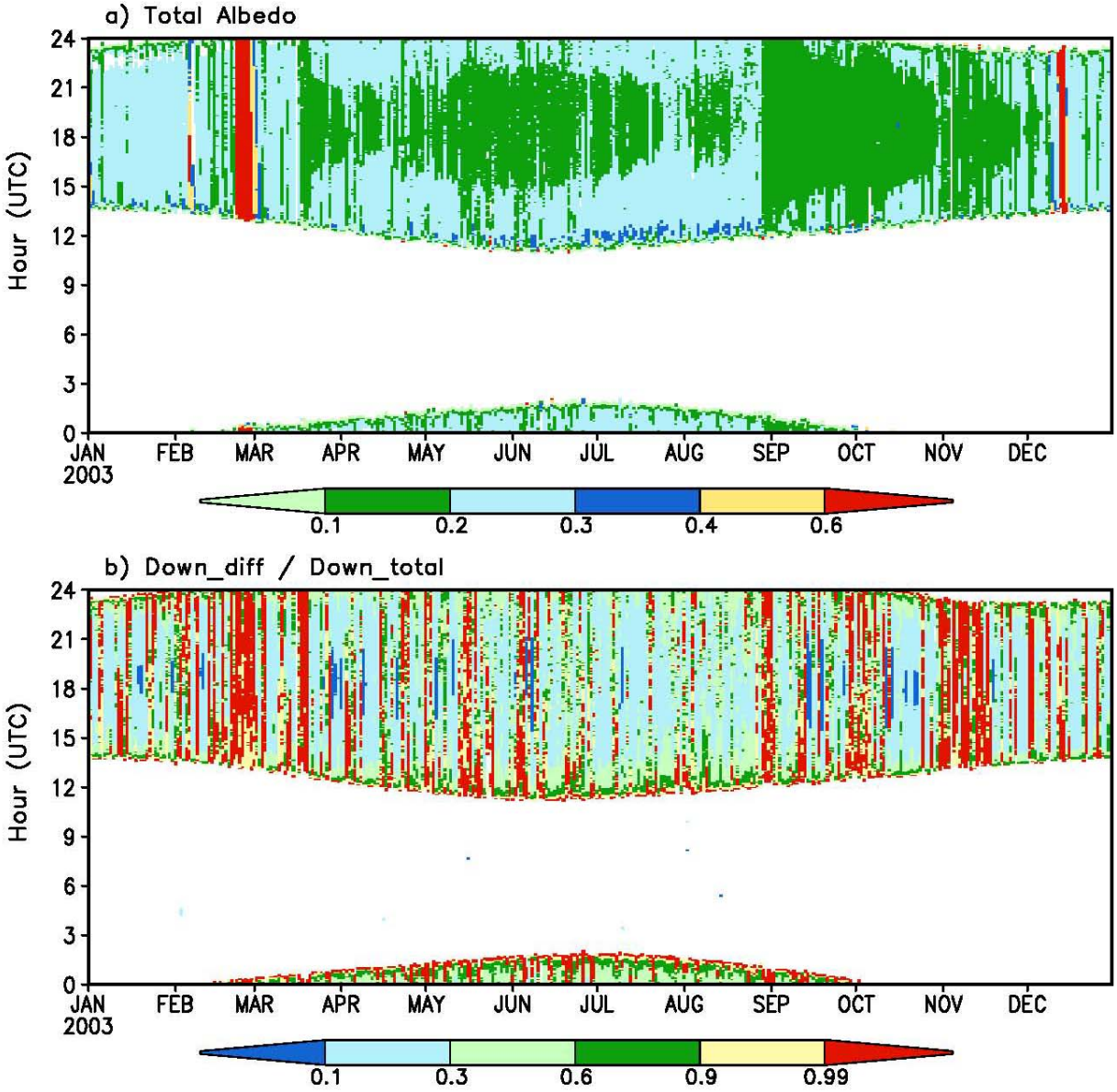

Figure 1. The diurnal and seasonal variations of a) surface albedo and b) the ratio between the downward diffuse and the downward total solar fluxes at the SGP CF in 2003. Here the albedo is for the solar flux that includes both the direct and diffuse beams. The temporal resolution of the data is five minutes.

Table 2. Total sample size of qualified five-minute mean data at the SGP CF site from the 1997-2004 period and the percent subgroup data used for various calculations.

Total samples	diffuse-beam albedo	clear-sky direct-beam albedo	all-sky direct-beam albedo	all-sky direct-beam albedo at SZA=60o	clear-sky direct-beam albedo at SZA=60o
245,606	15%	42%	75%	2.5%	1.3%

Diffuse-Beam Albedo at the SGP CF Site

It is known that the albedos for the direct and diffuse beams have different characteristics. The diffuse-beam albedo does not change with the SZA while the direct-beam albedo does. Therefore, it is necessary to treat the albedos differently. The ARM instruments measure surface downward total and diffuse-beam fluxes and the surface upward total flux. To derive the direct-beam and diffuse-beam albedos separately from the ARM data, one has to divide the measured upward flux into two parts: one associated with the downward direct beams and the other with the downward diffuse beams. A novel method is introduced here to first derive the diffuse-beam albedo.

Because of scattering by atmospheric constituents, the downward solar flux is composed of direct and diffuse beams. Usually, the diffuse part increases as the SZA increases and also increases as cloud amount increases. As an example, we show in Figure 1b the ratios between the downward diffuse-beam fluxes and the downward total fluxes at the SGP CF site in 2003. At many points the ratios were larger than 0.99 (red color in Figure 1b). These points scattered through the year and occurred at any time of the day. In other words, their occurrences were not biased towards any particular season or time of the day. Based on this observation, we chose a subset of the five-minute means for which the skies were overcast and the aforementioned ratios were larger than 0.99. The points satisfying these criteria accounted for 14.5% of all samples in 1997-2004. We performed two more tests by setting the critical ratio to 0.999 and 0.9999 and found no significant changes in the derived diffuse-beam albedos described below. We use here the 0.99 critical ratio to allow a lager sample size as a tradeoff for accuracy. We then calculated the (diffuse-beam) albedo as the ratio between the total upward and total downward fluxes from this subset. Figure 2 shows, for example, the distributions of the diffuse-beam albedo as a function of the cosine of SZA in January, April, July, and October, respectively. The most prominent feature is that, as expected, the diffuse-beam albedo does not vary with the SZA. However, considerable seasonal and annual variations occurred, which were probably caused by changes in the surface properties such as vegetation index and soil moisture amount. It is beyond the scope of this study to investigate these changes.

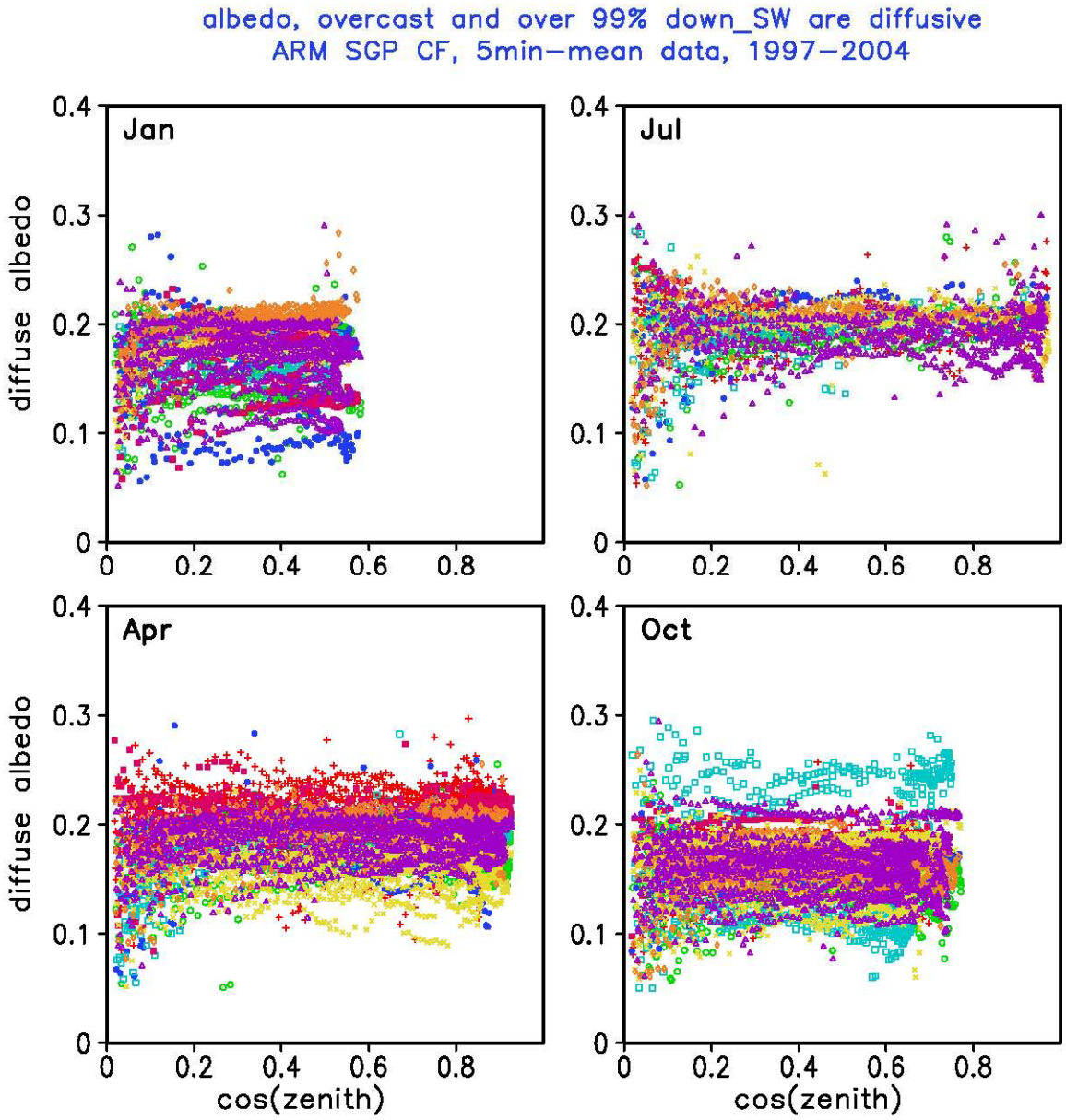

Figure 2. Distributions of surface diffuse-beam albedo against SZA in January, April, July, and October in 1997-2004 at the ARM SGP CF site. Different colors represent different years.

The albedos obtained above were then used to compute monthly-mean diffuse-beam albedo for each of the months in the eight years and the eight-year mean monthly albedos (Figure 3). It should be pointed out that these diffuse-beam albedos are based on spectrally integrated fluxes. In numerical models, diffuse-beam albedos are usually defined differently for the ultra-violet and visible band and for the near-infrared (NIR) band since surface albedo changes sharply from the visible to near-infrared spectrum for majority of land surface types (Li et al. 2002). In the NCEP GFS, the diffuse-beam albedo

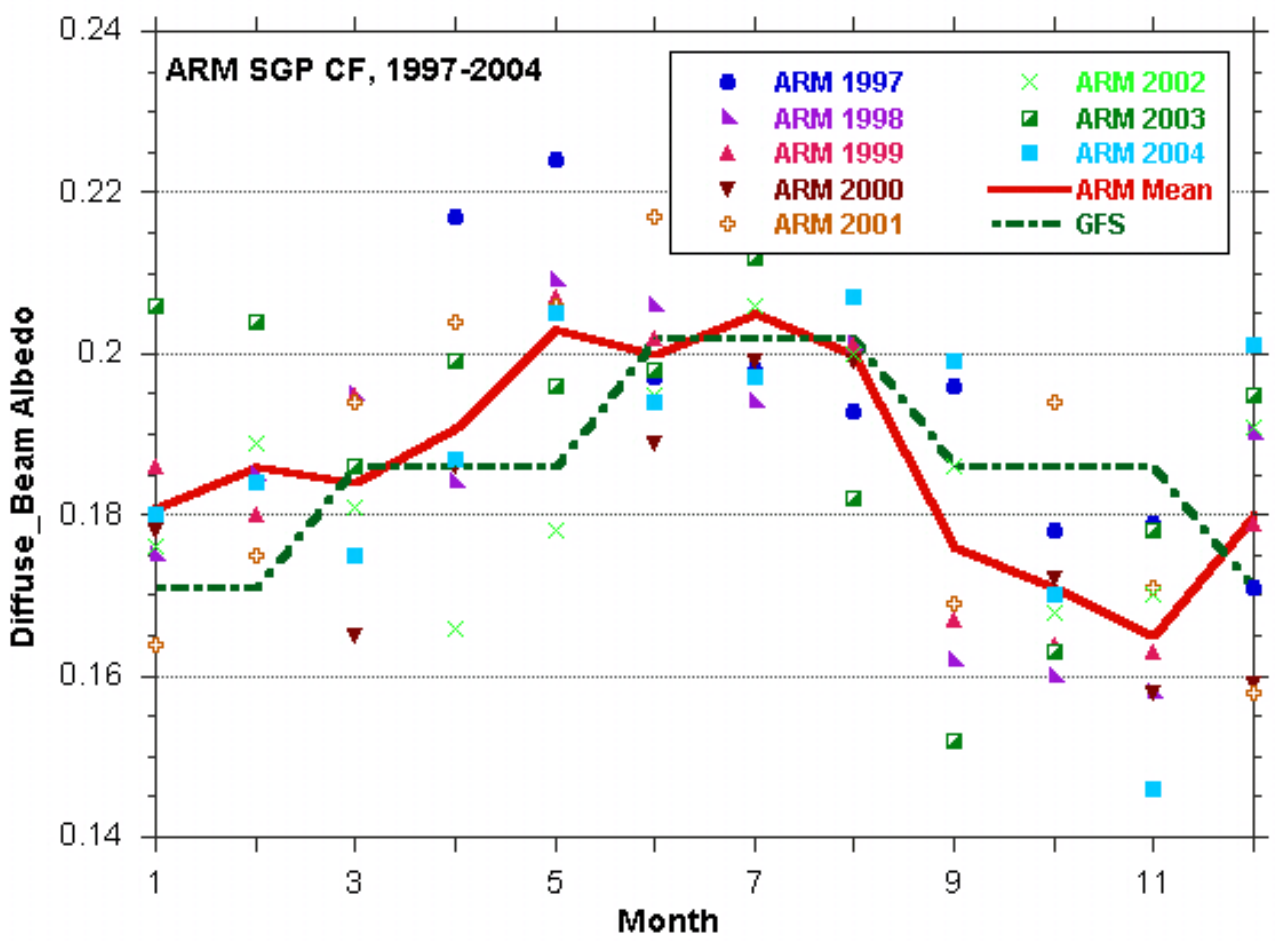

Figure 3. Monthly mean diffuse-beam albedos at the SGP CF derived from the ARM observations and the corresponding values prescribed in NCEP GFS.

$\alpha_{diff}(\lambda)$ in Eq. (2) is prescribed differently for each month and differently for the UUV and NIR bands (Hout et al. 2002). For comparison, we calculated spectrally-integrated diffuse-beam albedo by linearly combining the GFS two broadband albedos together with two weighting coefficients, each of which is the percent solar energy in each band relative to the solar constant as defined at the top of the atmosphere. The coefficient is 0.47047 for the UUV band and 0.52953 for the NIR band. These numbers may change slightly if defined for the solar flux at the surface depending on the shortwave absorption by the atmosphere at different wavelengths.

Figure 3 compares the spectrally-integrated monthly mean diffuse-beam albedos we derived from the ARM observations with those prescribed in the GFS. The numerical numbers are given in Table 3. The ARM monthly albedo has large year-to-year variations, probably due to changes in the surface properties. Nevertheless, the GFS monthly mean albedo is in good agreement with the 8-year mean

Table 3. Monthly mean surface albedos at the ARM SGP CF site. The ARM albedos are 1997-2004 means. Included in the parentheses are clear-sky albedos.

	GFS, Diffuse-Beam Albedo	ARM, Diffuse-Beam Albedo	ARM, Direct- Beam Albedo	ARM, Total Albedo	ARM, Direct-Beam Albedo at SZA=60°
Jan	0.171	0.181	0.254 (0.240)	0.206 (0.223)	0.232 (0.217)
Feb	0.171	0.186	0.238 (0.232)	0.204 (0.217)	0.227 (0.213)
Mar	0.186	0.184	0.234 (0.225)	0.201 (0.210)	0.228 (0.214)
Apr	0.186	0.191	0.232 (0.228)	0.205 (0.212)	0.229 (0.221)
May	0.186	0.203	0.233 (0.239)	0.211 (0.218)	0.242 (0.234)
Jun	0.202	0.200	0.241 (0.246)	0.212 (0.221)	0.249 (0.241)
Jul	0.202	0.205	0.236 (0.240)	0.215 (0.219)	0.241 (0.239)
Aug	0.202	0.200	0.247 (0.250)	0.217 (0.224)	0.251 (0.245)
Sep	0.186	0.176	0.230 (0.226)	0.194 (0.205)	0.231 (0.223)
Oct	0.186	0.171	0.245 (0.238)	0.199 (0.216)	0.228 (0.219)
Nov	0.186	0.165	0.237 (0.225)	0.193 (0.208)	0.224 (0.202)
Dec	0.171	0.180	0.239 (0.232)	0.205 (0.217)	0.210 (0.206)

ARM albedo. Both of them are larger in the northern summer months than in the northern winter months. The diffuse-beam albedo prescribed in the GFS seems to be too large for the September-October-November season.

Direct-Beam Albedo at the SGP CF Site

After obtaining the spectrally-integrated monthly mean diffuse-beam albedo (α_{diff}) for each month in the eight years, we calculated the part of upward solar fluxes ($F_{dir}^{\uparrow}$) that were associated with the downward direct-beam fluxes as

$$F_{dir}^{\uparrow} = F_{total}^{\uparrow} - \alpha_{diff}\left(F_{total}^{\downarrow} - F_{diff}^{\downarrow}\right), \tag{6}$$

where $F_{total}^{\downarrow}$, $F_{diff}^{\downarrow}$, and $F_{total}^{\uparrow}$ are the downward total shortwave (SW) flux, downward diffuse-beam SW flux and the upward total SW flux. These fluxes are from the ARM instrument measurements. Considering its large year-to-year variation, α_{diff} in each year was used for the calculation instead of the 8-year mean α_{diff}. Even though α_{diff} was derived from a subset of the observations under overcast conditions, the calculation was applied for all data samples under both clear and cloudy-sky conditions based on the assumption that α_{diff} does not change with the sky condition and only depends on the land surface type. Lyapustin (1999) showed that surface albedo is primarily an intrinsic property of surface characteristics and its dependence on atmospheric condition has a relatively minor effect.

For demonstration purposes, we show in Figure 4 the direct-beam albedo $\alpha_{dir}(\theta)$ as a function of SZA in January and July in 1997-2004 at the SGP CF using either all samples or only clear-sky samples for each month. On average, the sample size of the later is about 42% of the size of the former (Table 2). The

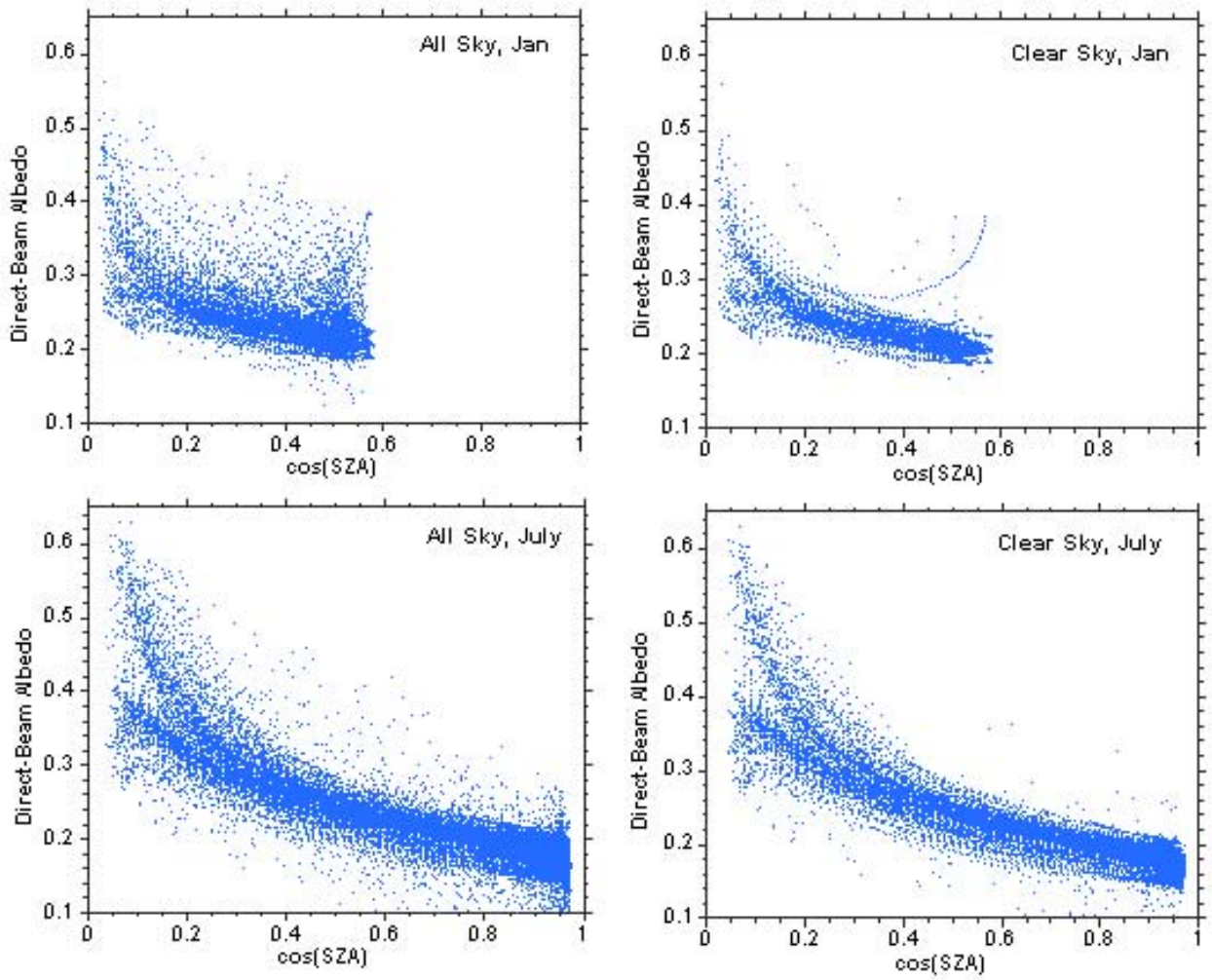

Figure 4. Direct-beam albedos in January (upper panels) and July (lower panels) derived from the ARM observations at the SGP CF using (7) for all-sky (left panels) and clear-sky (right panels) conditions.

distributions for the two cases are similar to each other. Their differences will be further quantified in the next section. Unlike the diffuse-beam albedo shown in Figure 2, the direct-beam albedo strongly depends on the SZA. In July, the albedo at sunrises and sunsets was two to three times larger than that at local noon. In the next section, we will make use of the diffuse-beam and direct-beam albedos presented in this section to evaluate the albedo parameterizations described in the introduction.

Normalized Direct-Beam Albedo and Its Parameterization

Parameterizations in the NCEP GFS and Derived from the MODIS Product

It has been known that the diffuse-beam albedo does not dependent on the SZA. We will no longer consider the parameterization given in Eq. (1), which was proposed for the total solar flux. The remaining investigation is focused on parameterizing the direct-beam albedo as a function of the SZA. The diffuse-beam and direct-beam albedos we obtained at the ARM SGP CF in previous sections are for the spectrally-integrated solar fluxes. The direct-beam albedos parameterized in Eqs. (2) – (5) are spectra dependent. Can we use the ARM measurements to evaluate these parameterizations? Here, we introduce the concept of normalized albedos. The NCEP GFS parameterization (Eq. 2) and the parameterizations Wang et al. (2006) derived from the MODIS data (Eqs. 3 and 4) can be rewritten as

$$N_{GFS} = \frac{\alpha_{dir}(\theta,\lambda)}{\alpha_{diff}(\lambda)} = \frac{1+d}{1+2d\cos(\theta)}, \tag{2a}$$

$$N_{W2} = \frac{\alpha_{dir}(\theta,\lambda)}{\alpha_{dir}(60^o,\lambda)} = 1 + B_1 \cdot \left[g_1(\theta) - g_1(60^o)\right] + B_2 \cdot \left[g_2(\theta) - g_2(60^o)\right], \tag{3a}$$

$$N_{W1} = \frac{\alpha_{dir}(\theta,\lambda)}{\alpha_{dir}(60^o,\lambda)} = \frac{1+c}{1+2c\cos(\theta)}. \tag{4a}$$

For a given surface type, the parameters d, B_1, B_2, and c are prescribed constants and they do not change with the solar spectrum. The normalized albedos are only functions of the SZA. Once these functions are determined and the spectra-dependent diffuse-beam albedo $\alpha_{diff}(\lambda)$ or the spectra-dependent direct-beam albedo $\alpha_{dir}(60°, \lambda)$ are given, the direct-beam albedos in different solar spectra bands can be calculated. The ARM SGP CF is covered by pasture and wheat. The corresponding values of the parameters given in Hou et al. (2002) and Wang et al. (2006) are $d = 0.4$, B_1 - 0.57, $B_2 = 0.12$, and $c = 0.26$. The functions $g_1(\theta)$ and $g_2(\theta)$ are described in Wang et al. (2006).

Since all the variables on the right-hand sides of Eqs. (2a) – (4a) do not depend on the solar spectrum, it can be easily proved that

$$\frac{\alpha_{dir}(\theta,\lambda)}{\alpha_{diff}(\lambda)} = \frac{\alpha_{dir}(\theta)}{\alpha_{diff}}, \tag{7}$$

$$\frac{\alpha_{dir}(\theta,\lambda)}{\alpha_{dir}(60^o,\lambda)} = \frac{\alpha_{dir}(\theta)}{\alpha_{dir}(60^o)}, \tag{8}$$

where the albedos on the left-hand sides are for solar fluxes in each broadband, and the albedos on the right-hand sides are for spectrally-integrated solar fluxes. This transformation allows us to use the ARM measured spectrally-integrated solar fluxes to assess the accuracy of the parameterized albedo-SZA relations.

The Liang et al. (2005) parameterization (Eq. 5) was structured differently from the ones above. The albedos over vegetation and bare soil are parameterized differently. The direct-beam albedo over bare soil not only depends on the SZA but also on soil moisture. Further, the coefficients C_1 and C_2 in Eq. (6) are prescribed different for the visible and near-infrared bands. Nevertheless, it will be shown that the normalized direct-beam albedo is still only a function of the SZA. First, we use Eq. (5) to deduce the direct-beam albedos at SZA=60° for the visible and the near-infrared band and denote them as $\alpha_{dir}^{vis}(\theta=60^o)=0.7275\alpha_{dir}^{vis}|_{\mu=0,\vartheta=0}F(\vartheta)$ and $\alpha_{dir}^{nir}(\theta=60^o)=0.7235\alpha_{dir}^{nir}|_{\mu=0,\vartheta=0}F^{nir}(\vartheta)$, respectively.

Then, dividing Eq. (5) by these two equations we have

$$N_{La}=\frac{\alpha_{dir}^{vis}(\theta)}{\alpha_{dir}^{vis}(\theta=60^o)}=1.3745-0.9869\cos(\theta)+0.4756\cos^2(\theta), \quad (5a.1)$$

$$N_{Lb}=\frac{\alpha_{dir}^{nir}(\theta)}{\alpha_{dir}^{nir}(\theta=60^o)}=1.3803-1.0104\cos(\theta)+0.4997\cos^2(\theta). \quad (5a.2)$$

One can see that the normalized albedos only change with the SZA. Although the normalization is performed separately for the visible and near-infrared bands, the difference between the two normalized albedos is relatively small (see Figure 6b). This reinforces that the normalized direct-beam albedo has weak dependence on the solar spectrum.

Fittings from the ARM Measurements at the SGP Site

Now that we have converted the parameterizations (Eqs. 2-5) for direct-beam albedos described in Hou et al. (2002), Wang et al. (2006), and Liang et al. (2005) into those (Eqs. 2a-5a) for the normalized direct-beam albedos, which only depend on the SZA, we will proceed to use the direct-beam and diffuse-beam albedos we derived from ARM measurements to assess the accuracy of these parameterizations. The focus is on how the normalized snow-free land surface albedo changes with SZA, especially at large SZA, and with or without clouds in the atmosphere.

Shown in Figure 5 are scatter plots of the normalized albedos $\alpha_{dir}(\theta)$ / α_{diff} and $\alpha_{dir}(\theta)$ / $\alpha_{dir}(60°)$ as functions of cos(θ) calculated using the ARM data for clear-sky and all-sky conditions, respectively. The calculations are carried out month by month for each year using all qualified samples of the

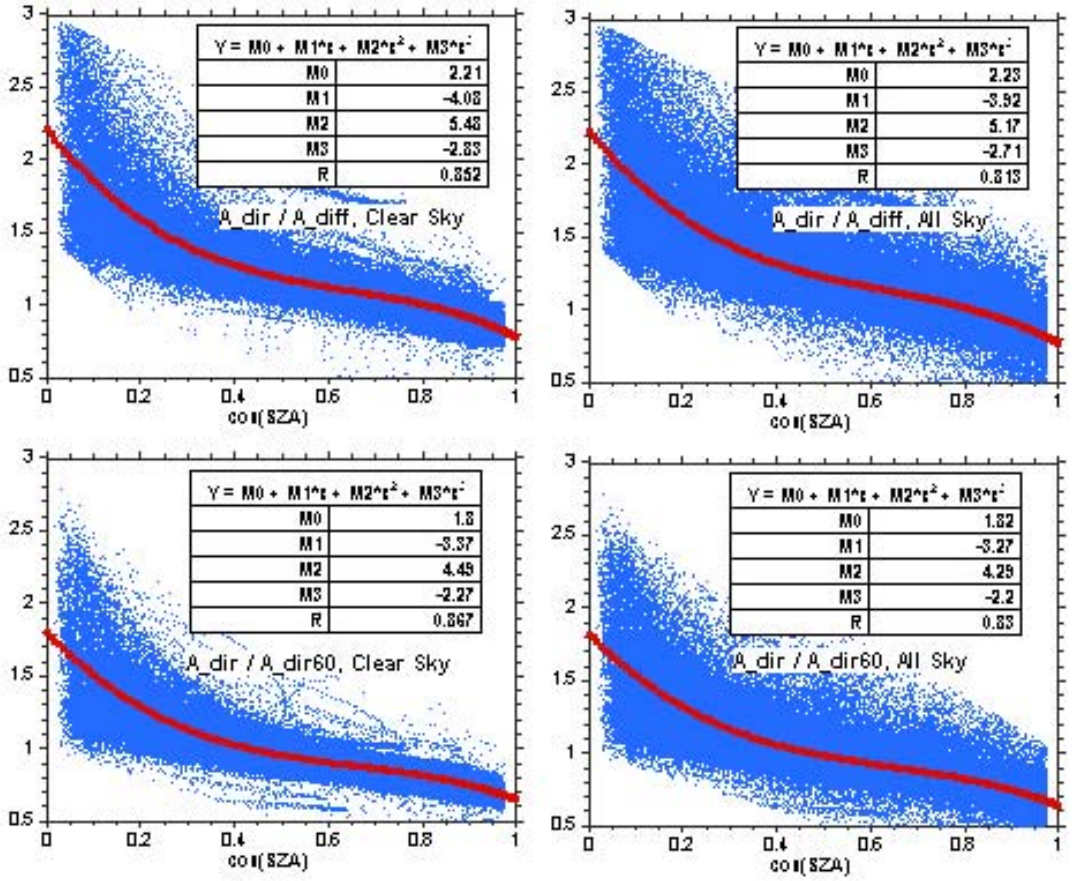

Figure 5. Scatter plots of direct-beam albedo that is either normalized by the diffuse-beam albedo (upper panels) or the direct-beam albedo at SZA=60^o (lower panels). The left (right) panels included clear-sky (all-sky) samples at the SGP CF in 1997-2004. In each panel, a third-order polynomial was fitted to the samples to show the empirical dependence of the normalized direct-beam albedo on the SZA.

direct-beam albedos $\alpha_{dir}(\theta)$ in each month and the corresponding monthly-mean α_{diff} and $\alpha_{dir}(60°)$. α_{diff} was obtained in the section titled, "Diffuse-Beam Albedo at the SGP CF Site" (Figure 3). We used samples of $\alpha_{dir}(\theta)$ that satisfy the condition $|\theta - 60°| \leq \Delta\theta$ in each month to compute the monthly mean $\alpha_{dir}(60°)$ for the clear-sky and all-sky cases, respectively. For $\Delta\theta$=1°, averaged for all years, 1.3% clear-sky samples and 2.5% all-sky samples satisfy this condition (Table 2). Table 3 gives the 1997-2004 mean monthly mean $\alpha_{dir}(60°)$ at the ARM SGP CF site. We tested the sensitivity of $\alpha_{dir}(60°)$ by doubling or halving $\Delta\theta$ and found little changes in $\alpha_{dir}(60°)$. Overall, the normalized direct-beam albedos in Figure 5 show strong dependence on SZA. The fitting for $\alpha_{dir}(\theta)$ / α_{diff} differs considerably from the fitting for $\alpha_{dir}(\theta)$ / $\alpha_{dir}(60°)$ because the monthly mean diffuse-beam albedo and direct-beam albedo at 60°are very different (see Table 3).

We included in each panel of Figure 5 all qualified samples of the normalized albedos in 1997-2004 at the SGP CF site and tested different fittings to obtain an empirical relation that best describes the dependence of the normalized direct-beam albedo on SZA. The third-order polynomial fitting was finally chosen for reducing fitting errors and for its similarity in format to the MODIS surface albedo retrieval algorithm (Schaaf et al. 2002). We had also performed additional polynomial fittings by using a subgroup of the samples that aimed at a particular year or a particular season for all years. The resultant fitting parameters did vary slightly with the volume of data used but showed no obvious dependence on the season or the year. We decided to maximize the use of samples at all time to obtain one fitting instead of multiple fittings for different seasons or months. Numerical models do not use different functions to parameterize the albedo-SZA relation for different seasons either.

Model Parameterizations versus ARM Fittings at the SGP CF Site

We now use the fittings derived from the ARM measurements to evaluate the accuracy of the parameterizations of (2a) – (5a). Shown in Figure 6a are the normalized direct-beam albedos $\alpha_{dir}(\theta)/\alpha_{diff}$ as a function of $\cos(\theta)$ as defined by the ARM fitting and the NCEP GFS parameterization (2a) for the SGP CF site. The ARM fittings for both the clear-sky and all-sky cases are presented. The difference between the two cases is small. Compared to the ARM fitting, the GFS parameterization underestimated the direct-beam albedo at all zenith angles. The largest bias occurs at sunrise and sunset times. Yang et al. (2006) found that in comparison with the ARM observations the surface downward shortwave fluxes at the SGP CF site from the NCEP GFS forecast were overestimated at all times of the day and the bias reached up to 50 W/m^2 at 3 p.m. local time. Coincidently, the upward shortwave fluxes from the forecasts matched rather well with the ARM observations. They pointed out that the discrepancy was probably attributable to inaccurate surface albedos prescribed in the GFS. The analysis described in the section titled, "Diffuse-Beam Albedo at the SGP CF Site," showed that the diffuse-beam albedo prescribed in the GFS was relatively accurate. Therefore, the discrepancy was caused the underestimate of the direct-beam albedo in the GFS.

Figure 6b compares the normalized direct-beam albedo $\alpha_{dir}(\theta)/\alpha_{dir}(60°)$ from the ARM fitting with those from the parameterizations (3a) – (5a). The most prominent feature is that the parameterizations Liang et al. (2005) and Wang et al. (2006) obtained using the MODIS BRDF data all tend to overestimate the direct-beam albedo for small zenith angles near local noon and largely underestimate the direct-beam albedo at large zenith angles at sunrises and sunsets. It has been known that the MODIS data are not accurate for SZA larger than 70° ($\cos(\theta) < 0.34$). However, it is not clear why these parameterizations all overestimate the albedo at small zenith angles. The constants in these parameterizations were obtained by minimizing the errors between the parameterized albedos and MODIS observed 16-day mean albedos (Liang et al. 2005; Wang et al. 2006). It is possible that this procedure led to an overestimate of the direct-beam albedo at small zenith angles as a compensation for the underestimate of the albedo at large zenith angles.

A few other points also can be drawn from Figure 6b. (1) Consistent with the fittings for $\alpha_{dir}(\theta)$ / α_{diff} in Figure 6a the fittings for $\alpha_{dir}(\theta)$ / $\alpha_{dir}(60°)$ are almost identical for the clear-sky and all-sky cases. The influence of atmospheric condition on the dependence of the surface-abledo on SZA is negligible. (2) Even though Wang et al. (2006) and Liang et al. (2005) took very different approaches to extract

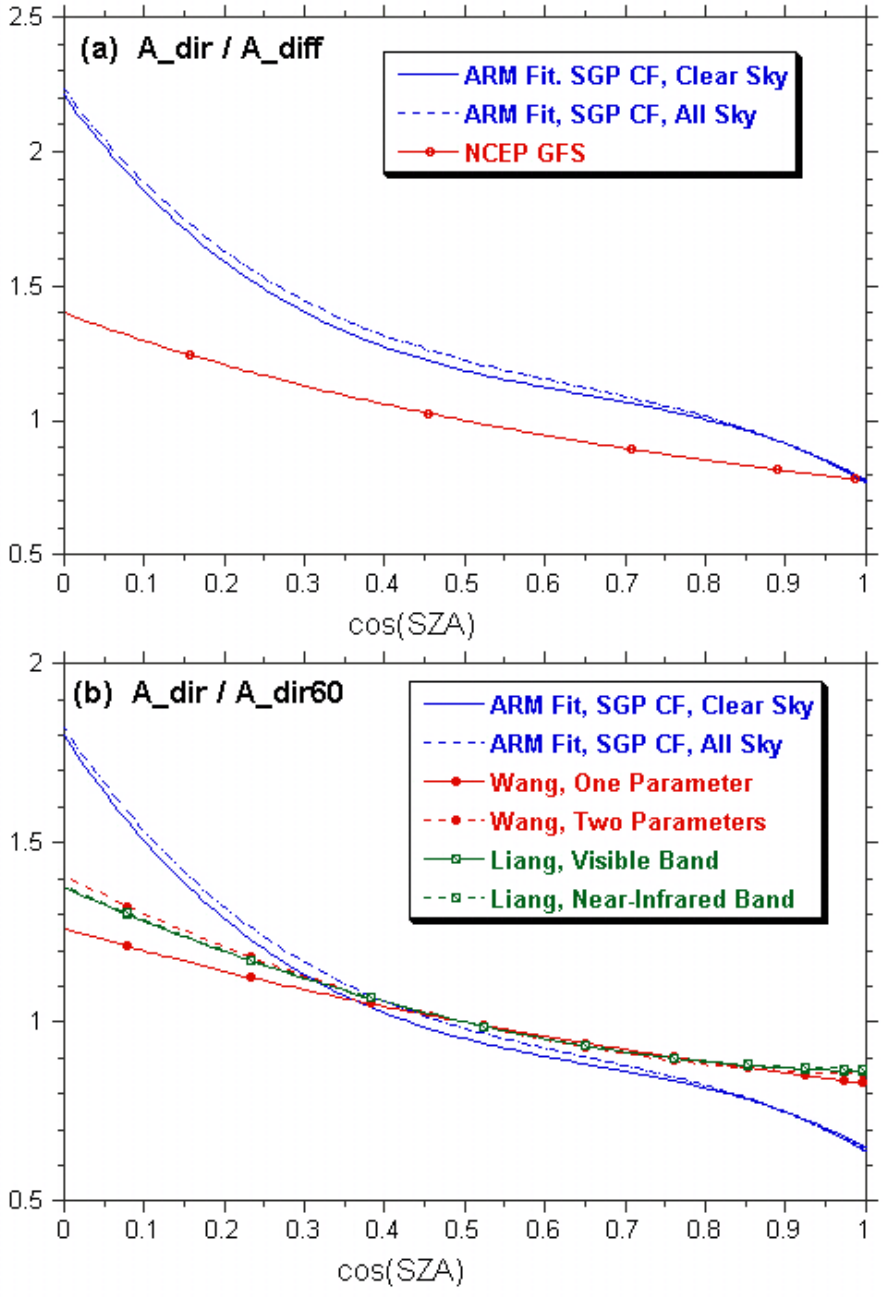

Figure 6. Dependence of normalized direct-beam albedo on SZA at the ARM SGP CF as determined by the ARM fittings in Figure 5 and by Eqs. (2a) – (5a). The direct-beam albedo is normalized by (a) the diffuse-beam albedo and (b) the direct-beam albedo at SZA=60°.

the dependence of the direct-beam albedo on SZA from the MODIS BRDF data, the two-parameter scheme (Eq. 3a) Wang et al. (2006) defined is almost identical to either of the schemes Liang et al. (2005) defined. (3) The normalized direct-beam albedos Liang et al. (2005) defined separately for the visible and near-infrared bands (Eqs. 5a.1 and 5a.2) show almost identical dependences on $\cos(\theta)$. Therefore, for model parameterizations it is acceptable to use only one function to describe the dependence of the normalized albedo on $\cos(\theta)$ for both spectra bands. The variation of the non-normalized direct-beam albedo with wavelength is represented by $\alpha_{dir}(60°, \lambda)$, which is prescribed differently for different spectra bands. (4) For the Wang et al. (2006) parameterizations, the one-parameter scheme is less accurate than the two-parameter scheme.

As an overall evaluation, we present in Figure 7 the percent errors of upward surface shortwave fluxes computed from the parameterizations of NCEP GFS and Wang et al. (2006) and the ARM fittings relative to the ARM-measured upward fluxes at the SGP CF site. The parameterizations of Liang et al. (2005) are excluded because of their dependence on soil moisture. All samples in the 1997-2004 period are included. The comparison based on only clear-sky samples gives similar results. The samples are divided into five bins, with $\cos(\theta)$ centered at 0.1, 0.3, 0.5, 0.7, and 0.9, respectively. The upward flux includes two parts, one associated with the downward diffuse beam and the other the downward direct beam. The first part is computed using the ARM measured downward diffuse beam and the monthly-mean diffuse-beam albedo prescribed in the GFS or the diffuse-beam albedo derived from the ARM observations (Figure 3 and Table 3). The second part is computed using the parameterizations of Eqs. (2a) – (4a) and the ARM fittings in Figure 5. Figure 7 shows that NCEP GFS parameterization underestimated the upward shortwave fluxes by about 15% at sunrises and sunsets and by about 10% at local noon times. The Wang et al. (2006) parameterizations gave rather an accurate estimate of daily mean fluxes, but underestimated the fluxes by a few percent at sunrises and sunsets and overestimated by a few percent at local noon time. The ARM fittings we obtained from this study improved the flux calculations.

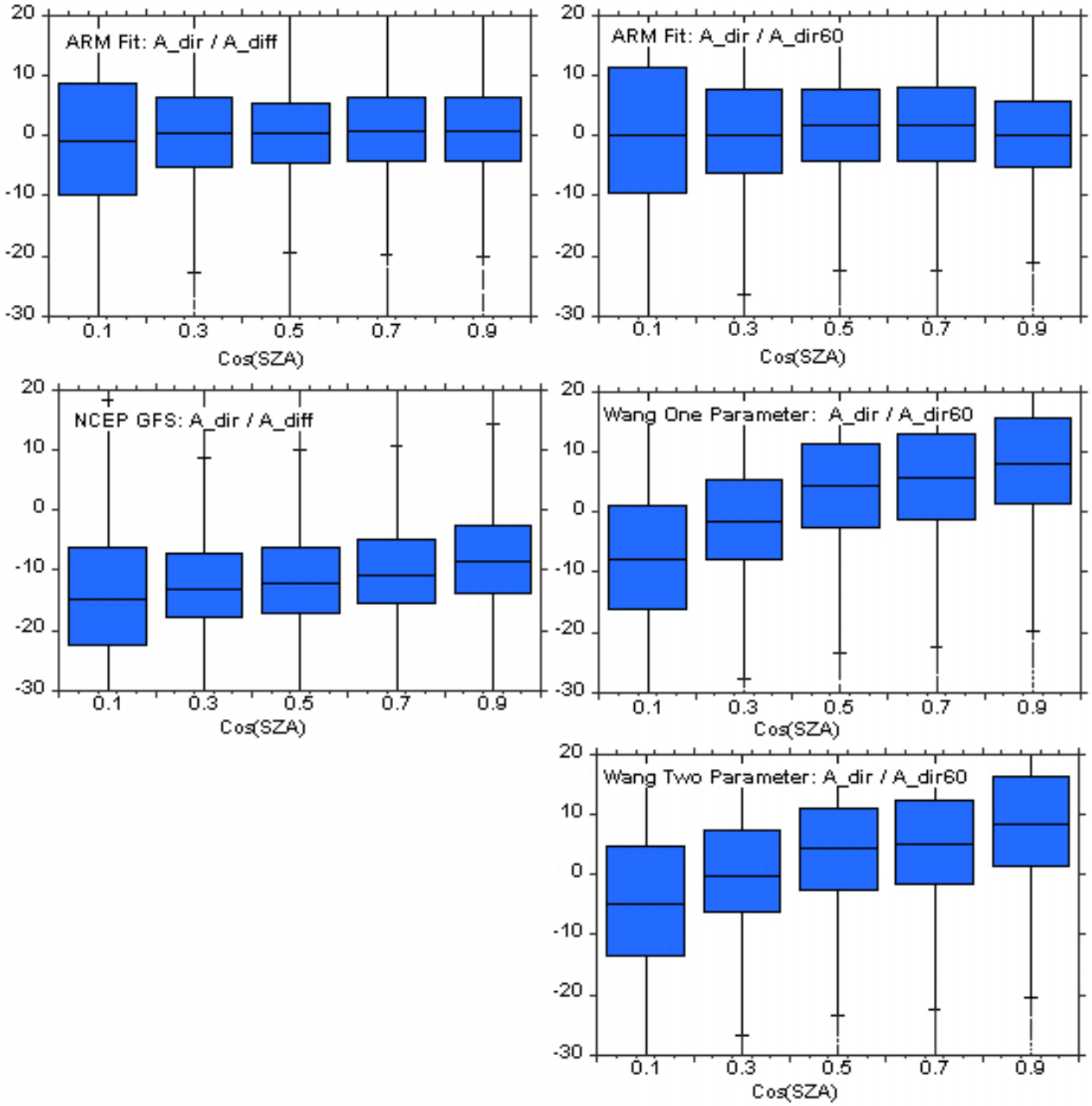

Figure 7. Box plots showing the percent errors of the upward shortwave flux, including both direct and diffuse beams, computed using the ARM fittings and the parameterizations of NCEP GFS and Wang et al. (2006), relative to those from the ARM observations at the SGP CF in 1997-2004.

University of the Relation between the Normalized Direct-Beam Albedo and SZA for Different Land Surface Types

Up to now the analyses are based on the single-point observations made at the SGP CF site. Are those empirical functions given in Figure 5 applicable for other land surface types at different locations? We will use of the ARM observations at the TWP Manus and Nauru islands to test if and how the results at these two sites may differ from those based on the SGP CF site.

Measurements of clouds and surface radiative fluxes available at the TWP Manus and Nauru islands are listed in Table 1. The instruments on Manus are situated on short grassland and those on Nauru are on bare soil. Following the same procedure described in previous sections the ARM measurements in 2001 – 2004 were used to compute the diffuse-beam and direct-beam albedos and to derive the fittings at the two sites that describe the dependences of the normalized direct-beam albedos on SZA for all-sky and clear-sky cases, respectively. The results for the all-sky and clear-sky cases are similar. We show in Figure 8a the all-sky fittings for $\alpha_{dir}(\theta)$ / α_{diff} and in Figure 8b the all-sky fittings for $\alpha_{dir}(\theta)$ / $\alpha_{dir}(60°)$. Fittings from earlier analyses for the SGP CF site and the parameterizations of Hou et al. (2002) and Wang et al. (2006) are also shown in Figure 8 for comparison.

The SGP CF is located in the middle latitude and is covered by pastures. The Manus and Nauru Islands are in the tropics and are covered by short grassland and bare soil, respectively. In spite of the different geographical locations and different surface types, the normalized direct-beam albedos on SZA at the three sites exhibit similar dependence on the SZA. The variation among the three ARM fittings is much smaller than the difference between any one of the fittings and the parameterization of NCEP GFS for $\alpha_{dir}(\theta)$ / α_{diff} or the parameterizations of Wang et al. (2006) for $\alpha_{dir}(\theta)$ / $\alpha_{dir}(60°)$.

We combined together all ARM observations at the SGP CF and the TWP Manus and Nauru Islands used in this study and derived two empirical functions (9) and (10) to describe the dependences of normalized direct-beam albedo on SZA. They are applicable for solar fluxes at the entire spectrum or at individual broadband since we have shown in previous sections that the parameterizations for the normalized direct-beam albedo have little variations among different spectra bands.

$$\alpha_{dir}(\theta,\lambda)/\alpha_{diff}(\lambda) = 2.287 - 3.374\cos(\theta) + 3.619\cos^2(\theta) - 1.603\cos^3(\theta), \quad (9)$$

$$\alpha_{dir}(\theta,\lambda)/\alpha_{dir}(60^o,\lambda) = 1.773 - 2.753\cos(\theta) + 3.053\cos^2(\theta) - 1.367\cos^3(\theta). \quad (10)$$

These two functions were obtained from three ARM sites. Their applicability for other surface types over the globe is not known. One ideal scenario is that the variations of the direct-beam albedo with surface type and/or geographical location are represented by the diffuse-beam albedo for the GFS-type parameterization and by $\alpha_{dir}(60°)$ for the Wang-type parameterizations, and that the normalized albedo

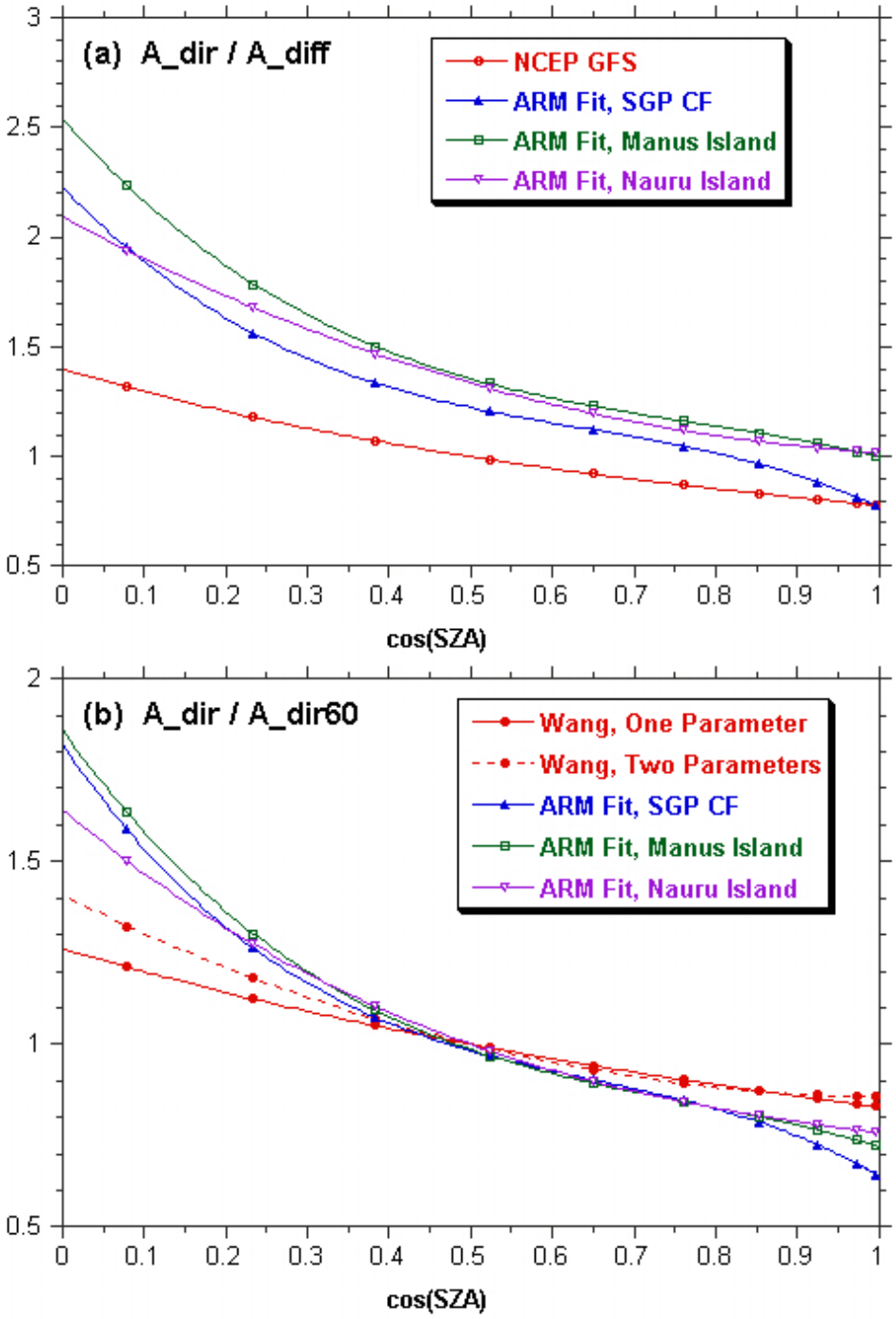

Figure 8. Dependences of the normalized direct-beam albedo on SZA as determined by the empirical fittings from the ARM measurements under all-sky conditions at the SGP CF, Manus Island, and Nauru Island, respectively. The parameterizations of NCEP GFS and Wang et al. (2006) are shown as well for references. The direct-beam albedo is normalized by (a) the diffuse-beam albedo and (b) the direct-beam albedos at SZA=60°.

only depends on the zenith angle. Then, in numerical models a single scheme that parameterizes the normalized direct-beam albedo as a function of SZA can be applied for all snow-free land surface types.

As we mentioned earlier, the coefficients B_1, B_2, and c in (3a) and (4a) Wang et al. (2006) obtained from the MODIS BRDF data were specified differently for 11 different land surface types. We used (3a) and (4a) to compute the normalized direct-beam albedos for all the 11 different land surface types with the coefficients given in Table 2 of Wang et al. (2006). The results are presented in Figures 9a and 9b, together with the normalized direct-beam albedo determined by the ARM-based fitting (10). One can see that the lines representing the 11 different surface types are clustered together, and are all distinctly different from the ARM-based fitting. Therefore, within a certain degree of accuracy it is probably practical to use one single function to parameterize the dependence of the normalized direct-beam albedo on the SZA for all land-surface types over the globe. The ARM-based fitting (10) is one such function, although its accuracy needs to be further tested with more ground-based observations that are of high solar angular resolution and are sampled over all surface types.

Summary and Discussion

In current climate and weather forecast models a diversity of methods are being used to parameterize land surface albedos. It has been know that the diffuse-beam albedo does not vary with the SZA. However, it is still not clear how the direct-beam albedo changes with the SZA. Many of the schemes such as those described in Briegleb et al. (1992) and Hou et al. (2002) are formulated following the one Dickson (1983) described for a specific land surface type. The parameterization coefficients of these schemes were obtained from limited observations. In recent years, significant progress has been made in the parameterization of land-surface albedo since the high-quality fine-resolution MODIS products became available. Wang et al. (2006) compared the direct-beam albedo parameterizations in a few current climate and weather forecast models and found large discrepancies between the model parameterizations and MODIS retrievals. Liang et al. (2005) also developed a new dynamical-statistical albedo scheme for snow-free land surfaces using the MODIS products. However, it is known that the MODIS data are not reliable near dust or dawn for SZA greater than 70° and they are 16-day composites retrieved under clear-sky conditions. The accuracy of these MODIS-based parameterizations also needs to be further tested using independent observations.

In this study we used the extensive and long-term ARM observations of surface solar radiative fluxes and cloud conditions at the SGP CF and TWP Manus and Nauru islands to evaluate the above albedo parameterizations. Because the ARM instruments only measured the surface downward total and diffuse solar fluxes and the surface reflected total flux, the monthly mean diffuse-beam albedo was first computed using the observations under overcast conditions when the downward total fluxes were all diffuse. The diffuse-beam albedo was then assumed to be invariant with atmospheric condition, and was used to divide the reflected total flux into two parts, one associated with the downward direct beam and the other with the downward diffuse beam for all observations. The direct-beam albedo was finally

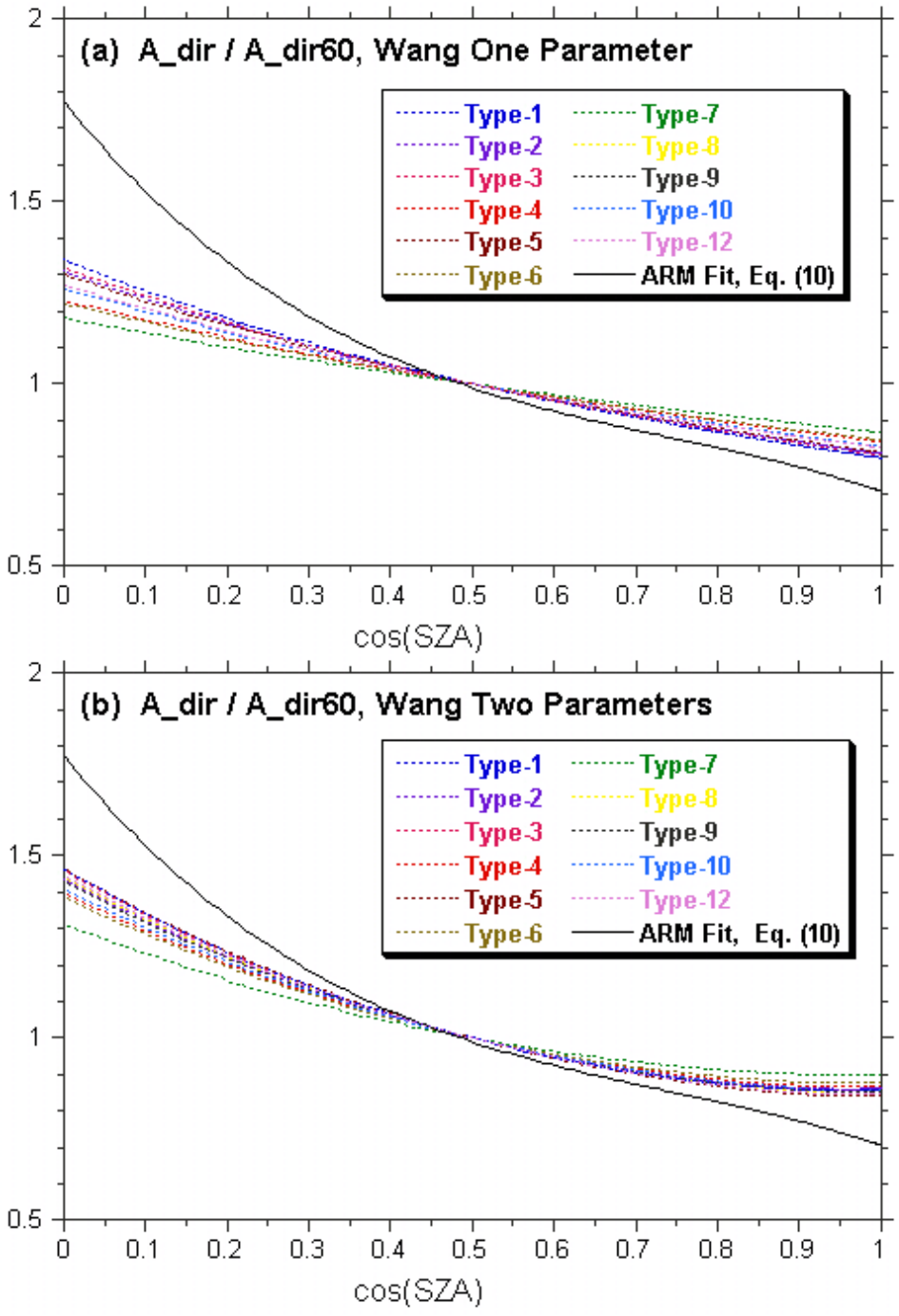

Figure 9. Dependences of the normalized direct-beam albedo on SZA as determined by the Wang et al. (2006) a) one-parameter and b) two-parameter fittings based on the MODIS BRDF product for 11 different land surface types (see Tables 1 and 2 of Wang et al. [2006]), and by the fitting (10) we obtained from three ARM sites (black unbroken line).

obtained using the first part of the reflected flux and the downward direct-beam flux. It was further normalized either by the diffuse-beam albedo or by the direct-beam albedo at SZA=60°. The normalized albedo only varies with the SZA and is independence of the solar spectrum.

Analyses of the ARM data showed that while the diffuse-beam albedo does not change with the SZA, the direct-beam albedo strongly depends on the SZA. The monthly mean diffuse-beam albedo prescribed in the GFS at the ARM SGP CF site matched closely to the multi-year mean monthly mean diffuse-beam albedo derived from the ARM observations. However, the direct-beam albedo parameterized in the GFS was underestimated at all zenith angles, with the largest errors found at the sunrise and sunset times. The parameterizations Liang et al. (2005) and Wang et al. (2006) derived from the MODIS data both underestimated the direct-beam albedo at large SZAs, probably because the MODIS product itself was not accurate at these angles, and slightly overestimated at local noon times. The analyses using only the ARM clear-sky samples or all samples under all-sky conditions led to almost identical results, indicating that the influence of atmospheric condition (cloud) on the surface albedo is relatively small in comparison to the large variation of the surface direct-beam albedo with the SZA.

It is interesting to point out that even though the normalized direct-beam albedo we reformulated from the Liang et al. (2005) parameterization was for bare-soil surface since Liang et al. (2005) treated separately the influence of soil moisture and canopy on the albedo, its dependence on the SZA has an almost identical distribution to that Wang et al. (2006) derived with all factors being folded into one index, e.g., the surface type. This led us to postulate that even though the direct-beam albedo itself varies with the SZA and surface conditions such as soil moisture, canopy and soil type, the normalized direct-beam albedo may be only a function of the SZA and has very week or no dependences on the other factors. If this is the case, a single equation that describes the dependence of the normalized direct-beam albedo on the SZA could be applied to all snow-free land surfaces over the globe for all seasons in climate and weather forecast models. The variations of the direct-beam albedo with the season and surface characteristics such as vegetation type and soil moisture (or geographical locations) were to be represented by the (normalization factor) denominator, e.g., the diffuse-beam albedo or the direct-beam albedo at SZA=60°, which can be derived from the MODIS product with high accuracy.

As a preliminary test, we analyzed the ARM observations made at the TWP Manus and Nauru islands and found the distributions of the normalized direct-beam albedo with SZA from these two island sites matched closely the distribution from the SGP CF site. The ARM instruments are situated on short grassland at the Manus site, bare soil on the Nauru site and on pastures at the SGP CF. The normalized direct-beam albedos that Wang et al. (2006) derived for 11 different land surface types from the MODIS product all exhibit similar dependences on the SZA. Irrelevant to the question that if the ARM-based parameterizations are more accurate than the MODIS-based ones, it is probably acceptable, within a certain degree of accuracy, to use a single function to parameterize the dependence of the normalized direct-beam albedo on the SZA for all land surface types. Of course, more ground observations that sample over different land surface types are required to prove or disprove this hypothesis. Nevertheless,

it is evident that the NCEP GFS parameterization and the MODIS-based schemes (Liang et al. 2005; Wang et al. 2006) all have large biases in comparison with any of the distributions derived from the three ACRF sites. This warrants further investigations on the parameterizations of the albedo-SZA relation in climate and weather forecast models.

Acknowledgments

Fanglin Yang was supported by the Office of Biological and Environmental Research of the U.S. Department of Energy as part of the Atmospheric Radiation Measurement Program postdoctoral fellowship at the National Centers for Environmental Prediction. He wishes to thank Wanda Ferrell at DOE and Stephen Lord at NCEP for their encouragement and support.

Contact

Fanglin Yang, 5200 Auth Road, Camp Springs, Maryland, email: fanglin.yang@noaa.gov, phone: 301-763-800 x7296.

References

Ackerman, T, and GM Stokes. 2003. "The atmospheric radiation measurement program." *Physics Today* 56:38–45.

Bonan, GB. 1996. A land surface model (LSM version 1.0) for ecological, hydrological, and atmospheric studies: Technical description and user's guide. NCAR Technical Note NCAR/TN-4171STR, 150 pp.

Briegleb, BP, P Minnis, V Ramanathan, and E Harrison. 1986. "Comparison of regional clear-sky albedos inferred from satellite observations and models comparisons." *Journal of Climate Applied Meteorological* 25:214–226.

Briegleb, B. 1992. "Delta–Eddington approximation for solar radiation in the NCAR Community Climate Model." *Journal of Geophysical Research* 97:7603–7612.

Clothiaux, EE, MA Miller, RC Perez, DD Turner, KP Moran, BE Martner, TP Ackerman, GG Mace, RT Marchand, KB Widener, DJ Rodriguez, T Uttal, JH Mather, CJ Flynn, KL Gaustad, and B Ermold. 2001. The ARM Millimeter Wave Cloud Radars (MMCRs) and the Active Remote Sensing of Clouds (ARSCL) Value Added Product (VAP), DOE Technical Memorandum, ARM VAP-002.1, U.S. Department of Energy, Washington D.C., 56 pp.

Dai, Y, X Zeng, RE Dickinson, I Baker, GB Bonan, MG Bosilovich, AS Denning, PA Dirmeyer, PR Houser, G-Y Niu, KW Oleson, CA Schlosser, and Z-L Yang. 2003. "The common land model." *Bulletin of the American Meteorological Society* 84:1013–1023.

Dai, Y, RE Dickinson, and Y-P Wang. 2004. "A two-big-leaf model for canopy temperature, photosynthesis and stomatal conductance." *Journal of Climate* 17:2281–2299.

Ek, MB, KE Mitchell, Y Lin, E Rogers, P Grunmann, V Koren, G Gayno, and JD Tarpley. 2003. "Implementation of the upgraded Noah land-surface model in the NCEP operational mesoscale Eta model." *Journal of Geophysical Research* 108(D22)8851.

Gao, F, C Schaaf, A Strahler, A Roesch, W Lucht, and R Dickinson. 2005. "The MODIS BRDF/Albedo climate modeling grid products and the variability of albedo for major global vegetation types." *Journal of Geophysical Reserch* 110:D01104.

Hou, Y-T, S Moorthi, and KA Campana. 2002. Parameterization of solar radiation transfer in the NCEP models, NCEP Office Note, 441, 34 pp.

Koster, RD, MJ Suarez, A Ducharne, M Stieglitz, and P Kumar. 2000. "A catchment-based approach to modeling land surface processes in a GCM, Part 1, model structure." *Journal of Geophysical Research* 105:24809–24822.

Li, Z, MC Cribb, and AP Trishchenko. 2002. "Impact of surface inhomogeneity on solar radiative transfer under overcast conditions." *Journal of Geophysical Research* 107(D16)4294.

Liang, X, M Xu, W Gao, K Kunkel, JR Slusser, Y Dai, Q Min, PR Houser, M Rodell, C Barker Schaaf, and F Gao. 2005. "Development of land surface albedo parameterization based on Moderate Resolution Imaging Spectroradiometer (MODIS) data." *Journal of Geophysical Research* 110:D11107.

Long, CN, and TP Ackerman. 1997. "Detection of clear skies using total and diffuse shortwave irradiance: Calculations of shortwave cloud forcing and clear sky diffuse ratio." In *Proceedings of the Sixth Atmospheric Radiation Measurement (ARM) Science Team Meeting*, CONF--9603149, U.S. Department of Energy, Washington, D.C.

Lyapustin, A. 1999. "Atmospheric and geometrical effects on land surface albedo." *Journal of Geophysical Research* 104:4127–4144.

Lucht, W, CB Schaaf, and AH Strahler. 2000. "An algorithm for the retrieval of albedo from space using semiempirical BRDF models." *IEEE Transactions of the Geosciences Remote Sensing* 38:977-998.

Matthews, E. 1983. "Global vegetation and land use: New high-resolution data bases for climate studies." *Journal of Climate and Applied Meteorology* 22:474–487.

Matthews, E. 1984. Vegetation, land-use, and seasonal albedo data sets: Documentation of archived data tape, NASA Technical Memorandum, 86107, National Aeronautics and Space Administration, Washington, D.C., 20 pp.

Minnis, P, S Mayor, WL Smith Jr., and DF Young. 1997. "Asymmetry in the diurnal variation of surface albedo." *IEEE Transactions on Geosciences and Remote Sensing* 35:879–891.

Mitchell, KE, D Lohmann, PR Houser, EF Wood, JC Schaake, A Robock, BA Cosgrove, J Sheffield, Q Duan, L Luo, RW Higgins, RT Pinker, JD Tarpley, DP Lettenmaier, CH Marchall, JK Entin, M Pan, W Shi, V Koren, J Mengm, BH Ramsay, and AA Bailey. 2004. "The multi-institution North American Land Data Assimilation System (NLDAS): Utilizing multiple GCIP products and partners in a continental distributed hydrological modeling system." *Journal of Geophysical Research* 109:D07S90.

Oleson, KW, Y Dai, G Bonan, M Bosilovich, R Dickinson, P Dirmeyer, F Hoffman, P Houser, S Levis, G-Y Niu, P Thornton, M Vertenstein, Z-L Yang, and X Zeng. 2004. Technical description of the Community Land Model (CLM), NCAR Technical Note NCAR/TN-461+STR, 174 pp.

Pinker, RT, and I Laszlo. 1992. "Modeling of surface solar irradiance for satellite applications on a global scale." *Journal of Applied Meteorology* 31:194–211.

Schaaf, CB, F Gao, AH Strahler, W Lucht, XW Li, T Tsang, NC Strugnell, XY Zhang, YF Jin, JP Muller, P Lewis, M Barnsley, P Hobson, M Disney, G Roberts, M Dunderdale, C Doll, RP d'Entremont, BX Hu, SL Liang, and JL Privette. 2002. "First operational BRDF, albedo and nadir reflectance products from MODIS." *Remote Sensing Environment* 83:135-148

Shi, Y, and CN Long. 2002. Best Estimate Radiation Flux Value Added Procedure: Algorithm Operational Details and Explanations, DOE Technical Memorandum, ARM-TR-008, U.S. Department of Energy, Washington D.C., 55 pp.

Stokes, GM, and SE Schwartz. 1994. "The Atmospheric Radiation Measurement (ARM) Program: programmatic background and design of the cloud and radiation test bed." *Bulletin of the American Meteorological Society* 75:1201–1221.

Trishchenko, A, Y Luo, Z Li, W Park, and K Khlopenkov. 2005. "Spectral, temporal and spatial properties of surface BRDF/Albedo over the ARM SGP area from multi-year satellite observations." In *Proceedings of the Fifteenth Atmospheric Radiation Measurement (ARM) Science Team Meeting*. Daytona Beach, Florida.

Wang, Z, X Zeng, M Barlage, RE Dickinson, F Gao, and CB Schaaf. 2004. Using MODIS BRDF/albedo data to evaluate global model land surface albedo." *Journal of Hydrometeorology* 5:3-14.

Wang. Z, X Zeng, and M Barlage. 2006. "MODIS BRDF-based land surface albedo parameterization for weather and climate models." *Journal of Geophysical Research* Accepted.

Yang, F, H-L Pan, S Krueger, S Moorthi, and S Lord. 2005. "Evaluation of the NCEP global forecast system at the ARM SGP site." *Monthly Weather Review* In Press.